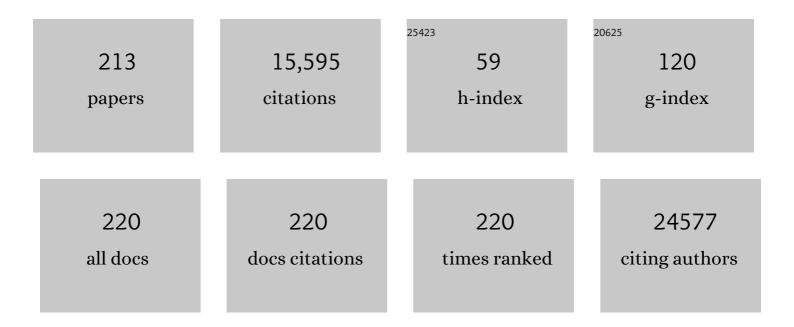
## Hyoyoung Lee

List of Publications by Year in descending order

Source: https://exaly.com/author-pdf/6238668/publications.pdf Version: 2024-02-01



HVOVOLING LEE

#	Article	IF	CITATIONS
1	Accelerating water reduction towards hydrogen generation via cluster size adjustment in Ru-incorporated carbon nitride. Chemical Engineering Journal, 2022, 429, 132282.	6.6	11
2	Selectively Regulating the Chiral Morphology of Amino Acid-Assisted Chiral Gold Nanoparticles with Circularly Polarized Light. ACS Applied Materials & Interfaces, 2022, 14, 3559-3567.	4.0	27
3	Unraveling the Function of Metal–Amorphous Support Interactions in Singleâ€Atom Electrocatalytic Hydrogen Evolution. Angewandte Chemie, 2022, 134, .	1.6	4
4	Unraveling the Function of Metal–Amorphous Support Interactions in Singleâ€Atom Electrocatalytic Hydrogen Evolution. Angewandte Chemie - International Edition, 2022, 61, .	7.2	62
5	Amorphization of Metal Nanoparticles by 2D Twisted Polymer for Super Hydrogen Evolution Reaction. Advanced Energy Materials, 2022, 12, .	10.2	26
6	Efficient ammonia synthesis <i>via</i> electroreduction of nitrite using single-atom Ru-doped Cu nanowire arrays. Chemical Communications, 2022, 58, 5257-5260.	2.2	17
7	Efficient ambient ammonia synthesis by Lewis acid pair over cobalt single atom catalyst with suppressed proton reduction. Journal of Materials Chemistry A, 2022, 10, 8432-8439.	5.2	11
8	Unveiling a Three Phase Mixed Heterojunction via Phaseâ€Selective Anchoring of Polymer for Efficient Photocatalysis. Advanced Energy Materials, 2022, 12, .	10.2	11
9	Amorphization of Metal Nanoparticles by 2D Twisted Polymer for Super Hydrogen Evolution Reaction (Adv. Energy Mater. 16/2022). Advanced Energy Materials, 2022, 12, .	10.2	0
10	Pseudo-capacitive and kinetic enhancement of metal oxides and pillared graphite composite for stabilizing battery anodes. Scientific Reports, 2022, 12, .	1.6	3
11	The effect of the dopant's reactivity for high-performance 2D MoS2 thin-film transistor. Nano Research, 2021, 14, 198-204.	5.8	9
12	Binder-free TiO2 hydrophilic film covalently coated by microwave treatment. Materials Chemistry and Physics, 2021, 258, 123884.	2.0	4
13	Unveiling surface charge on chalcogen atoms toward the high aspect-ratio colloidal growth of two-dimensional transition metal chalcogenides. Nanoscale, 2021, 13, 1291-1302.	2.8	2
14	Modulating Interfacial Charge Density of NiP <sub>2</sub> –FeP <sub>2</sub> via Coupling with Metallic Cu for Accelerating Alkaline Hydrogen Evolution. ACS Energy Letters, 2021, 6, 354-363.	8.8	146
15	Discovering ultrahigh loading of single-metal-atoms <i>via</i> surface tensile-strain for unprecedented urea electrolysis. Energy and Environmental Science, 2021, 14, 6494-6505.	15.6	79
16	Band restructuring of ordered/disordered blue TiO <sub>2</sub> for visible light photocatalysis. Journal of Materials Chemistry A, 2021, 9, 4822-4830.	5.2	17
17	Enhanced performance of Mo <sub>2</sub> P monolayer as lithium-ion battery anode materials by carbon and nitrogen doping: a first principles study. Physical Chemistry Chemical Physics, 2021, 23, 4030-4038.	1.3	26
18	Phase-selective active sites on ordered/disordered titanium dioxide enable exceptional photocatalytic ammonia synthesis. Chemical Science, 2021, 12, 9619-9629.	3.7	25

#	Article	IF	CITATIONS
19	Reducing the Photodegradation of Perovskite Quantum Dots to Enhance Photocatalysis in CO2 Reduction. Catalysts, 2021, 11, 61.	1.6	6
20	Identifying the Activity Origin of a Cobalt Singleâ€Atom Catalyst for Hydrogen Evolution Using Supervised Learning. Advanced Functional Materials, 2021, 31, 2100547.	7.8	93
21	Uncovering the Role of Countercations in Ligand Exchange of WSe <sub>2</sub> : Tuning the d-Band Center toward Improved Hydrogen Desorption. ACS Applied Materials & Interfaces, 2021, 13, 11403-11413.	4.0	15
22	Revealing the Synergy of Cation and Anion Vacancies on Improving Overall Water Splitting Kinetics. Advanced Functional Materials, 2021, 31, 2010718.	7.8	48
23	Energy/Charge Transfer Modulation with Spacer Ligands for Highly Emissive Quantum Dot–Polymer Blend. ACS Applied Materials & Interfaces, 2021, 13, 21534-21543.	4.0	3
24	Activity–Selectivity Enhancement and Catalytic Trend of CO <sub>2</sub> Electroreduction on Metallic Dimers Supported by N-Doped Graphene: A Computational Study. Journal of Physical Chemistry C, 2021, 125, 13176-13184.	1.5	12
25	Electrical characteristics of amyloid beta peptides in vertical junctions. NPG Asia Materials, 2021, 13, .	3.8	3
26	Doping-Mediated Lattice Engineering of Monolayer ReS <sub>2</sub> for Modulating In-Plane Anisotropy of Optical and Transport Properties. ACS Nano, 2021, 15, 13770-13780.	7.3	17
27	Unraveling the Synergy of Chemical Hydroxylation and the Physical Heterointerface upon Improving the Hydrogen Evolution Kinetics. ACS Nano, 2021, 15, 15017-15026.	7.3	59
28	A conjugated plier-linked nano-spacing graphite network for sodium-ion battery. Energy Storage Materials, 2021, 39, 70-80.	9.5	18
29	Covalently Bonded Ir(IV) on Conducted Blue TiO2 for Efficient Electrocatalytic Oxygen Evolution Reaction in Acid Media. Catalysts, 2021, 11, 1176.	1.6	3
30	Restructuring highly electron-deficient metal-metal oxides for boosting stability in acidic oxygen evolution reaction. Nature Communications, 2021, 12, 5676.	5.8	92
31	Present and Future of Phase-Selectively Disordered Blue TiO2 for Energy and Society Sustainability. Nano-Micro Letters, 2021, 13, 45.	14.4	8
32	Influence of lattice oxygen on the catalytic activity of blue titania supported Pt catalyst for CO oxidation. Catalysis Science and Technology, 2021, 11, 1698-1708.	2.1	18
33	Revealing well-defined cluster-supported bi-atom catalysts for enhanced CO <sub>2</sub> electroreduction: a theoretical investigation. Physical Chemistry Chemical Physics, 2021, 23, 25143-25151.	1.3	4
34	Layer-Dependent Band Structure of Ternary Metal Chalcogenides: Thickness-Controlled Hexagonal Feln <sub>2</sub> S <sub>4</sub> . Chemistry of Materials, 2021, 33, 164-176.	3.2	10
35	Moving beyond bimetallic-alloy to single-atom dimer atomic-interface for all-pH hydrogen evolution. Nature Communications, 2021, 12, 6766.	5.8	123
36	Single-Metal-Atom Dopants Increase the Lewis Acidity of Metal Oxides and Promote Nitrogen Fixation. ACS Energy Letters, 2021, 6, 4299-4308.	8.8	46

#	Article	IF	CITATIONS
37	Highly efficient nanostructured metal-decorated hybrid semiconductors for solar conversion of CO2 with almost complete CO selectivity. Materials Today, 2020, 35, 25-33.	8.3	44
38	Porosityâ€Engineering of MXene as a Support Material for a Highly Efficient Electrocatalyst toward Overall Water Splitting. ChemSusChem, 2020, 13, 945-955.	3.6	55
39	Boosting Electrocatalytic HER Activity of 3D Interconnected CoSP via Metal Doping: Active and Stable Electrocatalysts for pH-Universal Hydrogen Generation. Chemistry of Materials, 2020, 32, 9591-9601.	3.2	39
40	Efficient and Stable Solar Hydrogen Generation of Hydrophilic Rhenium-Disulfide-Based Photocatalysts <i>via</i> Chemically Controlled Charge Transfer Paths. ACS Nano, 2020, 14, 1715-1726.	7.3	50
41	Stabilizing the OOH* intermediate <i>via</i> pre-adsorbed surface oxygen of a single Ru atom-bimetallic alloy for ultralow overpotential oxygen generation. Energy and Environmental Science, 2020, 13, 5152-5164.	15.6	94
42	Highly Enhanced Photoelectrocatalytic Oxidation via Cooperative Effect of Neighboring Two Different Metal Oxides for Water Purification. Journal of Physical Chemistry C, 2020, 124, 11525-11535.	1.5	21
43	Frontispiece: Earthâ€Abundant Transitionâ€Metalâ€Based Bifunctional Electrocatalysts for Overall Water Splitting in Alkaline Media. Chemistry - A European Journal, 2020, 26, .	1.7	0
44	Highly stable multi-layered silicon-intercalated graphene anodes for lithium-ion batteries. MRS Communications, 2020, 10, 25-31.	0.8	4
45	Recent Developments of Advanced Ti3+-Self-Doped TiO2 for Efficient Visible-Light-Driven Photocatalysis. Catalysts, 2020, 10, 679.	1.6	28
46	Earthâ€Abundant Transitionâ€Metalâ€Based Bifunctional Electrocatalysts for Overall Water Splitting in Alkaline Media. Chemistry - A European Journal, 2020, 26, 6423-6436.	1.7	66
47	Understanding Surface Modulation to Improve the Photo/Electrocatalysts for Water Oxidation/Reduction. Molecules, 2020, 25, 1965.	1.7	8
48	Stable complete seawater electrolysis by using interfacial chloride ion blocking layer on catalyst surface. Journal of Materials Chemistry A, 2020, 8, 24501-24514.	5.2	102
49			

#	Article	IF	CITATIONS
55	Carbon-based asymmetric capacitor for high-performance energy storage devices. Electrochimica Acta, 2019, 300, 461-469.	2.6	19
56	Nanoparticle Linkerâ€Controlled Molecular Wire Devices Based on Double Molecular Monolayers. Small, 2019, 15, 1901183.	5.2	9
57	Phase-selective modulation of TiO2 for visible light-driven C H arylation: Tuning of absorption and adsorptivity. Molecular Catalysis, 2019, 471, 71-76.	1.0	5
58	Rapid oxygen diffusive lithium–oxygen batteries using a restacking-inhibited, free-standing graphene cathode film. Journal of Materials Chemistry A, 2019, 7, 10397-10404.	5.2	13
59	Feln <sub>2</sub> S <sub>4</sub> Nanocrystals: A Ternary Metal Chalcogenide Material for Ambipolar Fieldâ€Effect Transistors. Advanced Science, 2018, 5, 1800068.	5.6	18
60	Anion–Cation Double Substitution in Transition Metal Dichalcogenide to Accelerate Water Dissociation Kinetic for Electrocatalysis. Advanced Energy Materials, 2018, 8, 1702139.	10.2	70
61	Highly efficient hydrogen evolution catalysis based on MoS 2 /CdS/TiO 2 porous composites. International Journal of Hydrogen Energy, 2018, 43, 9307-9315.	3.8	38
62	Si-quantum-dot heterojunction solar cells with 16.2% efficiency achieved by employing doped-graphene transparent conductive electrodes. Nano Energy, 2018, 43, 124-129.	8.2	48
63	Low temperature solution synthesis of reduced two dimensional Ti <sub>3</sub> C <sub>2</sub> MXenes with paramagnetic behaviour. Nanoscale, 2018, 10, 22429-22438.	2.8	72
64	Preparation of Blue TiO2 for Visible-Light-Driven Photocatalysis. , 2018, , .		5
65	Facile C H arylation using catalytically active terminal sulfurs of 2 dimensional molybdenum disulfide. Tetrahedron Letters, 2018, 59, 3969-3973.	0.7	6
66	Hydrogen adsorption engineering by intramolecular proton transfer on 2D nanosheets. NPG Asia Materials, 2018, 10, 441-454.	3.8	16
67	An ultralight and flexible sodium titanate nanowire aerogel with superior sodium storage. Journal of Materials Chemistry A, 2018, 6, 17495-17502.	5.2	12
68	A molecular approach to an electrocatalytic hydrogen evolution reaction on single-layer graphene. Nanoscale, 2017, 9, 3969-3979.	2.8	38
69	Electrophoretic assembly and topological weaving of crumpled two-dimensional sheets with entangled defect loops. Carbon, 2017, 119, 211-218.	5.4	7
70	Activation of Ternary Transition Metal Chalcogenide Basal Planes through Chemical Strain for the Hydrogen Evolution Reaction. ChemPlusChem, 2017, 82, 785-791.	1.3	25
71	Bifunctional Oxygen Electrocatalysis through Chemical Bonding of Transition Metal Chalcogenides on Conductive Carbons. Advanced Energy Materials, 2017, 7, 1602217.	10.2	105
72	Superconductivity at 7.4 K in few layer graphene by Li-intercalation. Journal of Physics Condensed Matter, 2017, 29, 445701.	0.7	25

#	Article	IF	CITATIONS
73	Bulk <i>Ĵ²</i> -Te to few layered <i>Ĵ²</i> -tellurenes: indirect to direct band-Gap transitions showing semiconducting property. Materials Research Express, 2017, 4, 095902.	0.8	58
74	Activation of Ternary Transition Metal Chalcogenide Basal Planes through Chemical Strain for the Hydrogen Evolution Reaction. ChemPlusChem, 2017, 82, 1166-1166.	1.3	2
75	Functional Molecular Junctions Derived from Double Selfâ€Assembled Monolayers. Angewandte Chemie - International Edition, 2017, 56, 12122-12126.	7.2	16
76	Graphene-based composite electrodes for electrochemical energy storage devices: Recent progress and challenges. FlatChem, 2017, 6, 48-76.	2.8	27
77	Functional Molecular Junctions Derived from Double Selfâ€Assembled Monolayers. Angewandte Chemie, 2017, 129, 12290-12294.	1.6	2
78	Highly Efficient Thin-Film Transistor via Cross-Linking of 1T Edge Functional 2H Molybdenum Disulfides. ACS Nano, 2017, 11, 12832-12839.	7.3	19
79	Comparison of the Optical Properties of Graphene and Alkyl-terminated Si and Ge Quantum Dots. Scientific Reports, 2017, 7, 14463.	1.6	1
80	Highly Wrinkled and Porous Nitrogen Doped Graphene with High Electrochemical Activity for Supercapacitor. Science of Advanced Materials, 2017, 9, 30-33.	0.1	2
81	Flexible and Stretchable Optoelectronic Devices using Silver Nanowires and Graphene. Advanced Materials, 2016, 28, 4541-4548.	11.1	125
82	Tunable Bandgap Energy and Promotion of H <sub>2</sub> O <sub>2</sub> Oxidation for Overall Water Splitting from Carbon Nitride Nanowire Bundles. Advanced Energy Materials, 2016, 6, 1502352.	10.2	79
83	Mesoporous Non-stacked Graphene-receptor Sensor for Detecting Nerve Agents. Scientific Reports, 2016, 6, 33299.	1.6	17
84	Chemically modulated graphene quantum dot for tuning the photoluminescence as novel sensory probe. Scientific Reports, 2016, 6, 39448.	1.6	34
85	Graphene quantum dots and their possible energy applications: A review. Current Applied Physics, 2016, 16, 1192-1201.	1.1	185
86	Highly active and stable layered ternary transition metal chalcogenide for hydrogen evolution reaction. Nano Energy, 2016, 28, 366-372.	8.2	107
87	Catalyst-free bottom-up growth of graphene nanofeatures along with molecular templates on dielectric substrates. Nanoscale, 2016, 8, 17022-17029.	2.8	20
88	Impermeable flexible liquid barrier film for encapsulation of DSSC metal electrodes. Scientific Reports, 2016, 6, 27422.	1.6	7
89	Solar-light photocatalytic disinfection using crystalline/amorphous low energy bandgap reduced TiO2. Scientific Reports, 2016, 6, 25212.	1.6	61
90	Gate-dependent asymmetric transport characteristics in pentacene barristors with graphene electrodes. Nanotechnology, 2016, 27, 475201.	1.3	3

#	Article	IF	CITATIONS
91	Tunable Sub-nanopores of Graphene Flake Interlayers with Conductive Molecular Linkers for Supercapacitors. ACS Nano, 2016, 10, 6799-6807.	7.3	70
92	Highly transparent and flexible supercapacitors using graphene-graphene quantum dots chelate. Nano Energy, 2016, 26, 746-754.	8.2	179
93	Moving beyond flexible to stretchable conductive electrodes using metal nanowires and graphenes. Nanoscale, 2016, 8, 1789-1822.	2.8	69
94	Low-dimensional carbon and MXene-based electrochemical capacitor electrodes. Nanotechnology, 2016, 27, 172001.	1.3	48
95	An order/disorder/water junction system for highly efficient co-catalyst-free photocatalytic hydrogen generation. Energy and Environmental Science, 2016, 9, 499-503.	15.6	241
96	Highly Stretchable and Conductive Silver Nanoparticle Embedded Graphene Flake Electrode Prepared by In situ Dual Reduction Reaction. Scientific Reports, 2015, 5, 14177.	1.6	55
97	Reversible Switching Phenomenon in Diarylethene Molecular Devices with Reduced Graphene Oxide Electrodes on Flexible Substrates. Advanced Functional Materials, 2015, 25, 5918-5923.	7.8	39
98	Non-metal catalytic synthesis of graphene from a polythiophene monolayer on silicon dioxide. Carbon, 2015, 86, 272-278.	5.4	11
99	Light trapping by hydrothermally deposited zinc oxide nanostructures with high haze ratio. Materials Science in Semiconductor Processing, 2015, 37, 51-56.	1.9	9
100	High Mechanical and Tribological Stability of an Elastic Ultrathin Overcoating Layer for Flexible Silver Nanowire Films. Advanced Materials, 2015, 27, 2252-2259.	11.1	31
101	Generation of graphene quantum dots by the oxidative cleavage of graphene oxide using the oxone oxidant. New Journal of Chemistry, 2015, 39, 2425-2428.	1.4	36
102	Cylindrical nanostructured MoS <sub>2</sub> directly grown on CNT composites for lithium-ion batteries. Nanoscale, 2015, 7, 3404-3409.	2.8	86
103	Acid-free and oxone oxidant-assisted solvothermal synthesis of graphene quantum dots using various natural carbon materials as resources. Nanoscale, 2015, 7, 5633-5637.	2.8	85
104	Fast diffusion supercapacitors via an ultra-high pore volume of crumpled 3D structure reduced graphene oxide activation. RSC Advances, 2015, 5, 60914-60919.	1.7	23
105	Prevention of sulfur diffusion using MoS <sub>2</sub> -intercalated 3D-nanostructured graphite for high-performance lithium-ion batteries. Nanoscale, 2015, 7, 11928-11933.	2.8	23
106	Hybrid windshield-glass heater for commercial vehicles fabricated via enhanced electrostatic interactions among a substrate, silver nanowires, and an over-coating layer. Nano Research, 2015, 8, 1882-1892.	5.8	30
107	Enhancement of photodetection characteristics of MoS <sub>2</sub> field effect transistors using surface treatment with copper phthalocyanine. Nanoscale, 2015, 7, 18780-18788.	2.8	101
108	Fabrication of Nano Scale Electrode for Sensor Using Nanoimprint Lithography. Journal of Nanoelectronics and Optoelectronics, 2015, 10, 480-484.	0.1	1

#	Article	IF	CITATIONS
109	Synthesis of the Ni-doped ternary compound Ba(Fe <sub>1-x</sub> Ni <sub>x</sub> ) <sub>2</sub> Se <sub>3</sub> . Progress in Superconductivity and Cryogenics (PSAC), 2015, 17, 30-33.	0.3	2
110	Wellâ€Ordered and High Density Coordinationâ€Type Bonding to Strengthen Contact of Silver Nanowires on Highly Stretchable Polydimethylsiloxane. Advanced Functional Materials, 2014, 24, 3276-3283.	7.8	64
111	Mass Production of Graphene Quantum Dots by Oneâ€Pot Synthesis Directly from Graphite in High Yield. Small, 2014, 10, 866-870.	5.2	111
112	Vertical Alignments of Graphene Sheets Spatially and Densely Piled for Fast Ion Diffusion in Compact Supercapacitors. ACS Nano, 2014, 8, 4580-4590.	7.3	310
113	Facile preparation of an n-type reduced graphene oxide field effect transistor at room temperature. Chemical Communications, 2014, 50, 1224-1226.	2.2	41
114	A low ion-transfer resistance and high volumetric supercapacitor using hydrophilic surface modified carbon electrodes. Journal of Materials Chemistry A, 2014, 2, 6663-6668.	5.2	29
115	Fast synthesis of high-quality reduced graphene oxide at room temperature under light exposure. Nanoscale, 2014, 6, 11322-11327.	2.8	15
116	Optical properties of graphite oxide and reduced graphite oxide. Journal Physics D: Applied Physics, 2014, 47, 265306.	1.3	8
117	An Electrolyteâ€Free Flexible Electrochromic Device Using Electrostatically Strong Graphene Quantum Dot–Viologen Nanocomposites. Advanced Materials, 2014, 26, 5129-5136.	11.1	109
118	Cancer Therapy Using Ultrahigh Hydrophobic Drug-Loaded Graphene Derivatives. Scientific Reports, 2014, 4, 6314.	1.6	108
119	Facile Synthesis of Pt Nanoparticle and Graphene Composite Materials: Comparison of Electrocatalytic Activity with Analogous CNT Composite. Bulletin of the Korean Chemical Society, 2014, 35, 1973-1978.	1.0	0
120	High-Quality Reduced Graphene Oxide by a Dual-Function Chemical Reduction and Healing Process. Scientific Reports, 2013, 3, 1929.	1.6	236
121	Highly hydrophilic and insulating fluorinated reduced graphene oxide. Chemical Communications, 2013, 49, 8991.	2.2	59
122	Highly Bendable, Conductive, and Transparent Film by an Enhanced Adhesion of Silver Nanowires. ACS Applied Materials & Interfaces, 2013, 5, 9155-9160.	4.0	99
123	2D Graphene Oxide Nanosheets as an Adhesive Over-Coating Layer for Flexible Transparent Conductive Electrodes. Scientific Reports, 2013, 3, .	1.6	206
124	Performance enhancement of triisopropylsilylethynyl pentacene organic field effect transistors with inkjet-printed silver source/drain electrodes achieved via dispersible reduced graphene oxide. Thin Solid Films, 2013, 542, 327-331.	0.8	6
125	Nitrogen-Doped Partially Reduced Graphene Oxide Rewritable Nonvolatile Memory. ACS Nano, 2013, 7, 3607-3615.	7.3	67
126	Highly Sensitive and Selective Gas Sensor Using Hydrophilic and Hydrophobic Graphenes. Scientific Reports, 2013, 3, 1868.	1.6	178

#	Article	IF	CITATIONS
127	Graphene oxide as a recyclable phase transfer catalyst. Chemical Communications, 2013, 49, 5702.	2.2	39
128	Photo-switchable molecular monolayer anchored between highly transparent and flexible graphene electrodes. Nature Communications, 2013, 4, 1920.	5.8	119
129	Changes in major charge transport by molecular spatial orientation in graphene channel field effect transistors. Chemical Communications, 2013, 49, 6289.	2.2	11
130	Antiâ€Solvent Derived Nonâ€Stacked Reduced Graphene Oxide for High Performance Supercapacitors. Advanced Materials, 2013, 25, 4437-4444.	11.1	185
131	Voltage ontrolled Nonvolatile Molecular Memory of an Azobenzene Monolayer through Solutionâ€Processed Reduced Graphene Oxide Contacts. Advanced Materials, 2013, 25, 7045-7050.	11.1	42
132	Nonvolatile resistive memory of ferrocene covalently bonded to reduced graphene oxide. Chemical Communications, 2012, 48, 4235.	2.2	66
133	Dual Functions of Highly Potent Graphene Derivative–Poly- <scp>l</scp> -Lysine Composites To Inhibit Bacteria and Support Human Cells. ACS Nano, 2012, 6, 7151-7161.	7.3	141
134	A non-volatile memory device consisting of graphene oxide covalently functionalized with ionic liquid. Chemical Communications, 2012, 48, 913-915.	2.2	77
135	Dual n-type doped reduced graphene oxide field effect transistors controlled by semiconductor nanocrystals. Chemical Communications, 2012, 48, 4052.	2.2	19
136	Multilevel conductance switching for a monolayer of redox-active metal complexes through various metallic contacts. Journal of Materials Chemistry, 2012, 22, 1868-1875.	6.7	13
137	Binol salt as a completely removable graphene surfactant. Chemical Communications, 2012, 48, 7732.	2.2	54
138	Highly Airâ€Stable Phosphorusâ€Doped nâ€Type Graphene Fieldâ€Effect Transistors. Advanced Materials, 2012, 24, 5481-5486.	11.1	195
139	Synthesis of Highly nâ€Type Graphene by Using an Ionic Liquid. Chemistry - A European Journal, 2012, 18, 12207-12212.	1.7	41
140	Atomic Dopants Involved in the Structural Evolution of Thermally Graphitized Graphene. Chemistry - A European Journal, 2012, 18, 13466-13472.	1.7	20
141	A strategically designed porous iron–iron oxide matrix on graphene for heavy metal adsorption. Chemical Communications, 2012, 48, 9888.	2.2	106
142	Tuning of n―and pâ€Type Reduced Graphene Oxide Transistors with the Same Molecular Backbone. Chemistry - A European Journal, 2012, 18, 5155-5159.	1.7	23
143	nâ€Type Reduced Graphene Oxide Fieldâ€Effect Transistors (FETs) from Photoactive Metal Oxides. Chemistry - A European Journal, 2012, 18, 4923-4929.	1.7	23
144	Can Commonly Used Hydrazine Produce nâ€Type Graphene?. Chemistry - A European Journal, 2012, 18, 7665-7670.	1.7	39

#	Article	IF	CITATIONS
145	Solutionâ€Processed Reduced Graphene Oxide Films as Electronic Contacts for Molecular Monolayer Junctions. Angewandte Chemie - International Edition, 2012, 51, 108-112.	7.2	59
146	Thermal-Processing-Induced Structural Dynamics of Thiol Self-Assembly in Solution. Journal of Physical Chemistry C, 2011, 115, 15480-15486.	1.5	14
147	Highly qualified reduced graphene oxides: the best chemical reduction. Chemical Communications, 2011, 47, 9681.	2.2	67
148	Nonvolatile Memory Device Using Gold Nanoparticles Covalently Bound to Reduced Graphene Oxide. ACS Nano, 2011, 5, 6826-6833.	7.3	139
149	Electric field-induced nanopatterning of reduced graphene oxide on Si and a p–n diode junction. Journal of Materials Chemistry, 2011, 21, 5805.	6.7	13
150	One-pot reduction of graphene oxide at subzero temperatures. Chemical Communications, 2011, 47, 12370.	2.2	422
151	Selective patterning of ZnO nanorods on silicon substrates using nanoimprint lithography. Nanoscale Research Letters, 2011, 6, 159.	3.1	38
152	Nitronyl Nitroxide Radicals as Organic Memory Elements with Both n―and pâ€īype Properties. Angewandte Chemie - International Edition, 2011, 50, 4414-4418.	7.2	103
153	Non-volatile organic memory effect with thickness control of the insulating LiF charge trap layer. Organic Electronics, 2011, 12, 988-992.	1.4	12
154	Reduced graphene oxide by chemical graphitization. Nature Communications, 2010, 1, 73.	5.8	1,868
155	A photoswitchable methylene-spaced fluorinated aryl azobenzene monolayer grafted on silicon. Chemical Communications, 2010, 46, 5232.	2.2	27
156	Nonvolatile memory organic field effect transistor induced by the steric hindrance effects of organic molecules. Journal of Materials Chemistry, 2010, 20, 8016.	6.7	24
157	A HYSTERIC CURRENT/VOLTAGE RESPONSE OF REDOX-ACTIVE RUTHENIUM COMPLEX MOLECULES IN SELF-ASSEMBLED MONOLAYERS. , 2010, , 151-173.		0
158	Charge Storage Effect on In2O3Nanowires with Ruthenium Complex Molecules. Applied Physics Express, 2009, 2, 015001.	1.1	5
159	Molecular Monolayer Nonvolatile Memory with Tunable Molecules. Angewandte Chemie - International Edition, 2009, 48, 8501-8504.	7.2	70
160	Molecular Electron Transport Changes upon Structural Phase Transitions in Alkanethiol Molecular Junctions. ACS Nano, 2009, 3, 2469-2476.	7.3	30
161	Ferromagnetic Nanoscale Electron Correlation Promoted by Organic Spin-Dependent Delocalization. Journal of the American Chemical Society, 2009, 131, 18304-18313.	6.6	29
162	Adsorption of Azothiophene Dye Having an N-Bridging Bidentate Tail Group on Gold. Langmuir, 2009, 25, 10788-10793.	1.6	4

#	Article	IF	CITATIONS
163	Electron transport processes in on/off states of a single alkyl-tailed metal complex molecular switch. Journal of Materials Chemistry, 2009, 19, 7617.	6.7	19
164	Highâ€Fidelity Formation of a Molecularâ€Junction Device Using a Thicknessâ€Controlled Bilayer Architecture. Small, 2008, 4, 1399-1405.	5.2	24
165	Characterization of the tip-loading force-dependent tunneling behavior in alkanethiol metal–molecule–metal junctions by conducting atomic force microscopy. Ultramicroscopy, 2008, 108, 1196-1199.	0.8	9
166	Transformation of ZnTe nanowires to CdTe nanowires through the formation of ZnCdTe–CdTe core–shell structure by vapor transport. Journal of Materials Chemistry, 2008, 18, 875.	6.7	30
167	Molecular Conductance Switch-On of Single Ruthenium Complex Molecules. Journal of the American Chemical Society, 2008, 130, 2553-2559.	6.6	110
168	Quantum Interference in Radial Heterostructure Nanowires. Nano Letters, 2008, 8, 3189-3193.	4.5	26
169	Patterning of Conducting Polymers Using Charged Self-Assembled Monolayers. Langmuir, 2008, 24, 9825-9831.	1.6	21
170	Electrical breakdown and nanogap formation of indium oxide core/shell heterostructure nanowires. Nanotechnology, 2008, 19, 495702.	1.3	13
171	Statistical representation of intrinsic electronic tunneling characteristics through alkyl self-assembled monolayers in nanowell device structures. Journal of Vacuum Science & Technology B, 2008, 26, 904.	1.3	7
172	Selected Peer-Reviewed Articles from Molecular Electronics and Devices (ICMEAD 2007). Journal of Nanoscience and Nanotechnology, 2008, 8, 4520-4521.	0.9	0
173	Short-channel effect and single-electron transport in individual indium oxide nanowires. Nanotechnology, 2007, 18, 435403.	1.3	13
174	A statistical method for determining intrinsic electronic transport properties of self-assembled alkanethiol monolayer devices. Applied Physics Letters, 2007, 91, 253116.	1.5	20
175	Influence of metal-molecule contacts on decay coefficients and specific contact resistances in molecular junctions. Physical Review B, 2007, 76, .	1.1	67
176	Statistical analysis of electronic properties of alkanethiols in metal–molecule–metal junctions. Nanotechnology, 2007, 18, 315204.	1.3	111
177	Intermolecular Chain-to-Chain Tunneling in Metalâ^'Alkanethiolâ~'Metal Junctions. Journal of the American Chemical Society, 2007, 129, 3806-3807.	6.6	94
178	Rose Bengal Dye on Thiol-Terminated Bilayer for Molecular Devices. Langmuir, 2007, 23, 5195-5199.	1.6	11
179	Charge Transport of Alkanethiol Self-Assembled Monolayers in Micro-Via Hole Devices. Journal of Nanoscience and Nanotechnology, 2006, 6, 3487-3490.	0.9	6
180	Molecular chain-to-chain tunneling and nanowell devices for electronic transport studies in metal- alkanethiol-metal junctions. , 2006, , .		0

#	Article	IF	CITATIONS
181	Development of molecular logic array and memory device. , 2006, , .		1
182	Fabrication of Nanosized Molecular Array Device and Logic Gate Using Dimethyl-Phenylethynyl Thiol. Journal of Nanoscience and Nanotechnology, 2006, 6, 3470-3473.	0.9	9
183	An Enhanced Grid Scheduling with Job Priority and Equitable Interval Job Distribution. Lecture Notes in Computer Science, 2006, , 53-62.	1.0	6
184	Fabrication of Nanosized Molecular Array Device and Logic Gate Using Dimethyl-Phenylethynyl Thiol. Journal of Nanoscience and Nanotechnology, 2006, 6, 3470-3473.	0.9	4
185	Fabrication of nanosized molecular array device and logic gate using dimethyl-phenylethynyl thiol. Journal of Nanoscience and Nanotechnology, 2006, 6, 3470-3.	0.9	2
186	Charge transport of alkanethiol self-assembled monolayers in micro-via hole devices. Journal of Nanoscience and Nanotechnology, 2006, 6, 3487-90.	0.9	0
187	Solution-Processible Blue-Light-Emitting Polymers Based on Alkoxy-Substituted Poly(spirobifluorene). ETRI Journal, 2005, 27, 181-187.	1.2	21
188	Synthesis and Photoluminescent Properties of Violet Emitting 5,6-Diphenylfuro[2,3-d]pyrimidine Derivatives ChemInform, 2005, 36, no.	0.1	0
189	Effect of GaN Microlens Array on Efficiency of GaN-Based Blue-Light-Emitting Diodes. Japanese Journal of Applied Physics, 2005, 44, L18-L20.	0.8	25
190	Transport mechanism of self-assembled D-σ-A-thiol monolayers in metal-molecule-metal structure. Synthetic Metals, 2005, 152, 293-296.	2.1	4
191	Discotic liquid crystalline materials for potential nonlinear optical applications: synthesis and liquid crystalline behavior of 1,3,5-triphenyl-2,4,6-triazine derivatives containing achiral and chiral alkyl chains at the periphery. Tetrahedron Letters, 2004, 45, 1019-1022.	0.7	72
192	Synthesis of regio- and stereoselective alkoxy-substituted spirobifluorene derivatives for blue light emitting materials. Tetrahedron, 2003, 59, 2773-2779.	1.0	40
193	Organic blue light emitting materials based on spirobifluorene. Current Applied Physics, 2003, 3, 469-471.	1.1	17
194	Organic field-effect transistors using perylene. Optical Materials, 2003, 21, 439-443.	1.7	39
195	Pentacene thin film transistors fabricated on plastic substrates. Synthetic Metals, 2003, 139, 445-451.	2.1	54
196	Mechanisms of Exchange Modulation in Trimethylenemethane-type Biradicals:  The Roles of Conformation and Spin Density. Journal of the American Chemical Society, 2003, 125, 15426-15432.	6.6	62
197	Deep-level defect characteristics in pentacene organic thin films. Applied Physics Letters, 2002, 80, 1595-1597.	1.5	145
198	Electronic defect characteristics of pentacene organic thin films deposited on SiO 2 /Si substrates. ,		0

2002, 4464, 352.

#	Article	IF	CITATIONS
199	Singletâ~'Triplet Gap in Triplet Ground-State Biradicals Is Modulated by Substituent Effects. Journal of the American Chemical Society, 2002, 124, 10054-10061.	6.6	49
200	Charge Distribution in Bis-Dioxolene Radical Metal Complexes. Synthesis and DFT Characterization of Dinuclear Co(III) and Cr(III) Complexes with a Mixed-Valent,S=1/2Semiquinone-Catecholate Ligand. Inorganic Chemistry, 2001, 40, 1582-1590.	1.9	58
201	Molecular Structures of Carbonyl-Linked Bis(dioxolene) Complexes:Â Can a Carbonyl Group Act as an Effective Ferromagnetic Coupler?. Inorganic Chemistry, 2001, 40, 546-549.	1.9	15
202	Ferromagnetically Coupled Bis(semiquinone) Ligand Enforces High-Spin Ground States in Bis-metal Complexes. Inorganic Chemistry, 2001, 40, 408-411.	1.9	60
203	Synthesis of a Nanoporous Polymer with Hexagonal Channels from Supramolecular Discotic Liquid Crystals. Angewandte Chemie - International Edition, 2001, 40, 2669-2671.	7.2	111
204	A homochiral metal–organic porous material for enantioselective separation and catalysis. Nature, 2000, 404, 982-986.	13.7	3,805
205	Synthesis and characterization of a planarized, trimethylenemethane-type bis(semiquinone) biradical. Tetrahedron, 1999, 55, 12079-12086.	1.0	17
206	Cross-Conjugated Bis(porphryin)s:Â Synthesis, Electrochemical Behavior, Mixed Valency, and Biradical Dication Formation. Journal of Organic Chemistry, 1999, 64, 9124-9136.	1.7	45
207	Structureâ^'Property Relationships in Trimethylenemethane-Type Biradicals. 2. Synthesis and EPR Spectral Characterization of Dinitroxide Biradicalsâ€. Journal of Organic Chemistry, 1999, 64, 4386-4396.	1.7	39
208	Electronic Properties of Bisporphyrin Biradical Dications. Molecular Crystals and Liquid Crystals, 1999, 334, 459-467.	0.3	3
209	A Modified Procedure for Sonogashira Couplings:  Synthesis and Characterization of a Bisporphyrin, 1,1-Bis[zinc(II) 5â€~-ethynyl-10â€~,15â€~,20†-trimesitylporphyrinyl]methylenecyclohexane. Journal of Organic Chemistry, 1998, 63, 4034-4038.	1.7	71
210	Oxidation of a Bis[Zn(II) porphyrin] Yields a Nondisjoint, Exchange-Coupled π Dication-Biradical. Journal of Organic Chemistry, 1998, 63, 7584-7585.	1.7	20
211	Unsymmetrical Dialkyl Sulfides for Self-Assembled Monolayer Formation on Gold:Â Lack of Preferential Cleavage of Allyl or Benzyl Substituents. Chemistry of Materials, 1998, 10, 4148-4153.	3.2	13
212	Synthesis and Characterization of Phenylnitroxide-Substituted Zinc(II) Porphyrins. Journal of Organic Chemistry, 1998, 63, 769-774.	1.7	47
213	7-Amino-2-pyrenecarboxylic Acid. Journal of Organic Chemistry, 1996, 61, 5481-5484.	1.7	23